



Small-scale turbulence can reduce parasite infectivity to dinoflagellates

Gisela Llaveria¹, Esther Garcés¹, Oliver N. Ross², Rosa Isabel Figueroa¹,
Nagore Sampedro¹, Elisa Berdalet^{1,*}

¹Institut de Ciències del Mar and ²Unitat de Tecnologia Marina, CSIC, Passeig Marítim de la Barceloneta, 37-49, 08003 Barcelona, Spain

ABSTRACT: Small-scale turbulence and parasite infection are 2 important factors that govern the dynamics and fate of phytoplankton populations. We experimentally investigated the influence of turbulent mixing on the infectivity of the parasite *Parvilucifera sinerae* to dinoflagellates. Natural phytoplankton communities were collected during 3 stages of a bloom event in Arenys de Mar Harbour (NW Mediterranean). The 15 to 60 µm size fraction was used as the inoculum and distributed into spherical flasks. Half of the recipients were exposed to turbulence while the rest were kept still. In the experiments, the dinoflagellate assemblage was mainly composed of *Prorocentrum micans*, *Scrippsiella trochoidea* and *Alexandrium minutum*. We observed a collapse of *A. minutum* and *S. trochoidea* populations in the unshaken flasks, which coincided with an increase in parasite infectivity. After a short exposure to turbulence, the development of the dinoflagellate populations slowed down and stabilised as expected. In the shaken treatments, the infectivity was lower and the decay in the host cells numbers was delayed compared to the still treatments. The degree of interference of the turbulence with infectivity varied among the experiments, due to differences in cell abundances and possibly their physiological state. Results from a numerical model suggest that turbulence could lead to a 25 to 30 % decrease in the maximum infection rate, which could be due to host population dispersion and/or reduced host–parasite contact times. Turbulence may thus be effective in delaying the initial infection, but not in preventing it.

KEY WORDS: Dinoflagellates · Infectivity · *Parvilucifera sinerae* · Parasite · Small-scale turbulence · Sporangia · Numerical model

— Resale or republication not permitted without written consent of the publisher —

INTRODUCTION

The dynamics of phytoplankton communities is driven by a wide range of interactions between biological and environmental factors at different spatial and temporal scales. Hydrodynamic and meteorological forcings can lead to the accumulation or dispersal of microalgal cells by advection, modify phytoplankton sinking and buoyancy patterns, alter their exposure to light and nutrient availability and contribute to the selection of ‘life forms’ (Margalef 1978). At small scales, turbulence directly affects different physiological processes of phytoplankton cells, such as nutri-

ent uptake, that may influence the size structure and species composition of the community (e.g. Kjørboe 1993, Estrada & Berdalet 1997, Arin et al. 2002, Maar et al. 2002). Small-scale turbulence particularly affects dinoflagellate physiology (e.g. growth rates, cell division, asexual encystment, toxin production), which could influence their blooming capacity (e.g. revision by Berdalet & Estrada 2005, Bolli et al. 2007, Llaveria et al. 2009). Furthermore, by interfering with particles and plankton encounter rates (Rothschild & Osborn 1988) turbulence can modulate different behavioural aspects of the microorganisms (sexual reproduction, parasite infection, grazing) that in turn

*Corresponding author. Email: berdalet@icm.csic.es

play a key role in the proliferation of the different species.

Interestingly, several studies have suggested that parasites (viruses, bacteria or eukaryotes) could control (harmful) phytoplankton (e.g. Nishitani et al. 1985, Bruning et al. 1992, Kim et al. 1998). Montagnes et al. (2008) noted that parasitic infection could even be a more effective mechanism of dinoflagellate bloom control than microzooplankton grazing. At present, research is focussed on the taxonomic identification (using novel molecular tools) of different dinoflagellate parasites and, if possible, on their life cycle as well. This is the case, for instance, for the eukaryotic phylum Perkinsozoa, which includes several species, e.g. *Parvilucifera infectans* (Norén et al. 1999) and *P. sinerae* (Figueroa et al. 2008), with the capacity to specifically infect dinoflagellates. This group of parasites has 2 well defined stages in its life cycle: (1) a free-living stage as a very small flagellated zooid with an elongated body, about 2 to 4 µm long, which is difficult to recognize by optical microscopy, and (2) as a sporangium inside a host cell. The presence of a dark cyst inside the host cell is indicative of mature sporangia. This advanced stage of cellular infection is identified by optical microscopy, and its abundance can be used as an estimator of the parasite infectivity (Figueroa et al. 2008). This knowledge may facilitate further progress towards a better understanding of the factors that could modulate host–parasite dynamics in phytoplankton. In lakes, it has been observed that epidemics of chytrids on diatom populations coincided with periods of increased turbulence (Doggett & Porter 1996 and references therein). This feature could be due in part to the resuspension of fungal resting spores from the sediment. Turbulence could also enhance host–parasite contact rates, analogously to increased predator–prey encounter rates (Rothschild & Osborn 1988, Saiz et al. 1992, Alcaraz 1997). However, increased encounter rates may not necessarily lead to higher ingestion rates (Peters & Marrasé 2000), at least when turbulence intensities are high (Mackenzie et al. 1994). In the same line, Kühn & Hofmann (1999) noted that the encounter rate between host diatoms and the zoospores of a parasitoid nanoflagellate increased with turbulence, but the contact time was reduced. The authors hypothesised that turbulence interfered with the chemotactic signals, making it more difficult for a parasite to locate a host. Indeed, other factors, such as sensory or behavioural characteristics (migration, feeding activity), could also be involved in regulating encounter dynamics under natural conditions (e.g. Kjørboe & Visser 1999, Peters & Marrasé 2000). The present study deals with a possible control mechanism of phytoplankton populations: the infection by a parasite.

The main objective of the present work was to explore whether (and if so, how) turbulence affects parasite infection of dinoflagellates. To address this question, we collected field samples during 3 distinct and temporally separated phases of a phytoplankton spring bloom, characterised by the presence of *Prorocentrum micans*, *Scrippsiella trochoidea* and the toxic *Alexandrium minutum*, as well as the parasite *Parvilucifera sinerae*, which has the capacity to infect the latter 2 dinoflagellate species. We then subjected the samples to laboratory-generated turbulence (using the same experimental setup as in previous studies on turbulence–dinoflagellate interactions; Berdalet et al. 2007, Bolli et al. 2007, Llaveria et al. 2009) or kept them unperturbed. We compared the 2 treatments in terms of dinoflagellate cell abundances and data on the infectivity by *P. sinerae*. Furthermore, we recorded changes in the number of ecdysal cysts (hereafter referred to as pellicle cysts based on Bravo et al. 2010) and resting cysts to explore whether these life forms could represent a defence mechanism against the parasite infection, as was suggested for pellicle cysts in a previous study on *A. ostenfeldii* and the parasite *P. infectans* (Toth et al. 2004). Finally, we used a simple numerical infectivity model to help evaluate our observations.

MATERIALS AND METHODS

General design and setup. Previous studies have shown recurring dinoflagellate spring blooms in Arenys de Mar Harbour, 50 km north of Barcelona (Vila et al. 2001, Van Lenning et al. 2007). This site is included in the harmful algal blooms regional monitoring programme of the Catalan Water Agency (ACA), which provides periodic information on the main noxious organisms in the area. For the present study, additional samples were collected in Arenys de Mar Harbour since 1 February 2006 to track the evolution of the entire phytoplankton community. On 28 February, and 10 and 29 March 2006 (Fig. 1), sample volumes of the *in situ* phytoplankton community were used as inocula for what will subsequently be referred to as Expts I, II and III. Given that phytoplankton communities change along the temporal succession of a bloom, they cannot be considered replicates, but they help us evaluate the consistency of our results. In the laboratory, the communities were screened through a 60 µm diameter mesh to eliminate most micro-zooplankton and large diatoms. Nanoplankton was removed by a second screening, using a 15 µm diameter mesh. Thus for each of the 3 inocula, we used the 15 to 60 µm phytoplankton size fraction. In each of the 3 experiments, the inoculum was distributed into 4 Florence flasks (spher-

ical Pyrex vessels with flat bottom) of 4 l capacity, ensuring that each flask contained similar concentrations of *Alexandrium minutum*, which we chose as a reference species due to its toxicogenic capacity and its sensitivity to turbulence observed in previous studies (Berdalet et al. 2007, Bolli et al. 2007). Commensurate with the protocol and set-up used in these works, we started Expts II and III with an *A. minutum* concentration of about 500 cells ml⁻¹. However, in Expt I, due to the low concentration of dinoflagellates in the natural community, the screening process took long and used a high volume of sample. Nevertheless, we could only achieve a concentration of 150 *A. minutum* cells ml⁻¹ in the inoculum. Autoclaved seawater was then added to the inoculum in each flask so the total liquid content was at the 3 l mark. Inorganic nutrients and vitamins were supplied to obtain a final concentration corresponding to an f/20 seawater enriched medium (Guillard 1975). As in Bolli et al. (2007), all 4 experimental flasks were kept still during the first 3 d following inoculation. Thereafter, 2 of these flasks were randomly chosen to be subjected to turbulence on an orbital shaking table at 120 rpm, with a 30 mm orbit diameter, over 10 d. For each experiment, we thus had 2 replicates that were kept still for the entire duration of the experiment, serving as controls, and 2 replicates that from Day 4 onward underwent the turbulence treatment on the orbital shakers. We will refer to these 2 different treatments as 'Still' and 'Turbulent', respectively. With this configuration of the orbital shaker, the experimentally generated turbulence had an average

kinetic energy dissipation rate (ϵ) of ca. 27 cm² s⁻³ (2.7 × 10⁻¹ W kg⁻¹), as estimated by a miniaturised acoustic Doppler velocimeter. A scheme of the setup used to perform \times estimations can be found in Fig. 1 of Berdalet et al. (2007). A complete description of the calculations was provided by Guadayol et al. (2009).

The experiments were carried out in a culture chamber with a controlled light:dark (L:D) cycle of 12:12 h (light period starting at 08:00 h local time), temperature (18–20°C) and irradiance (110–120 μ mol photons m⁻² s⁻¹). For technical reasons, it was not possible to set the experimental temperature to the *in situ* conditions (12.6–13°C). This should not have had a large effect on the growth capacities of the phytoplankton, however, given their worldwide occurrence and their broad temperature tolerance range (e.g. see the global distribution of strain collection sites at the Provasoli-Guillard National Center for Culture of Marine Phytoplankton [CCMP]: <https://ccmp.bigelow.org/node/55>). All chosen experimental settings matched those used by Bolli et al. (2007) and Llaveria et al. (2009), who studied the effects of turbulence on the physiology of *Alexandrium minutum*, which allows for a direct comparison between the results.

Every 2 to 3 d, at 12:00 h (i.e. 4 h after the onset of the light period), we took a sample from each flask and measured the different parameters. Samplings were performed without opening the flasks and without stopping the shaking in the Turbulent treatment. The Florence flasks had a cotton plug pierced by an L-shaped glass tube connected to a Teflon tube holding a stopcock at the end. The glass tube reached 1 cm above the bottom of the Florence flask. Fifteen ml of the culture were discarded, as they corresponded to the volume retained along the tube by hydrostatic pressure and thus were not representative of the cells exposed to the treatment. In the Still flasks, the distribution of the cells was patchy: cysts settled at the bottom of the container, and motile cells performed nictemeral migrations. To obtain representative samples, the Still flasks were gently shaken before sampling. Mixing prevented the formation of layers of high cell concentration in the Turbulent treatments.

Cellular abundance of the most common dinoflagellate species. Samples were fixed with Lugol's iodised solution. The phytoplankton communities in the field samples collected from 1 February to 15 April (Fig. 1) were characterised on an inverted microscope using sedimentation chambers (Utermöhl 1958). Samples (50 or 10 ml, depending on the cell abundance) were allowed to settle for 24 h, and phytoplankton cells were subsequently enumerated in an appropriate area (over the entire chamber surface or along transects) depending on the cell densities (Utermöhl 1958 as illustrated in Fig 4.2 of Throndsen 1995) using a Leica-

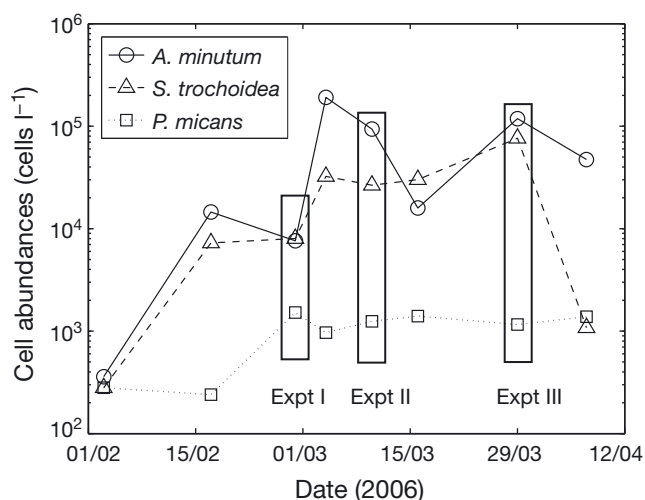


Fig. 1. *Alexandrium minutum*, *Scrippsiella trochoidea*, and *Prorocentrum micans*. Temporal evolution of cellular abundances of the 3 species which dominated the natural dinoflagellate population in Arenys de Mar Harbour during the 2006 spring bloom. The 3 rectangles indicate the dates when the inocula of the natural community were obtained for Expts I, II & III, respectively

Leitz DM-II inverted bright field microscope with at a 200 to 400× magnification. The different taxa were identified according to Balech (1995) and Steidinger & Tangen (1997). In the experiments, the abundances of the dominant dinoflagellate species (*Prorocentrum micans*, *Alexandrium minutum*, and *Scrippsiella trochoidea*) were estimated with the 1 ml capacity Sedgewick-Rafter counting cell slides. A minimum of 400 cells of each species were counted. When the cell concentration was below this threshold, samples were processed by the Utermöhl (1958) method in 10 ml sedimentation chambers.

Infectivity of *Parvilucifera sinerae*. The presence of the parasite is clearly detected when mature sporangia are identified by the presence of a dark cyst inside the dinoflagellate cells (Figuerola et al. 2008). Accordingly, to evaluate the virulence of parasite infection over the duration of the experiments, the abundance of mature sporangia was used as a proxy for the number of infected cells (Figuerola et al. 2008). In this experiment, only *Alexandrium minutum* and *Scrippsiella trochoidea* showed signs of infection, but not *Prorocentrum micans*. Thus, the infectivity is defined as the ratio of infected *A. minutum* and *S. trochoidea* cells (I) to the total combined cell number from both species:

$$\text{Infectivity}(\%) = \frac{I}{S+I} \times 100 \quad (1)$$

where S denotes susceptible cells, i.e. those cells that are not recognised as mature sporangia and are considered susceptible to become infected by the parasite.

Mature sporangia of *Parvilucifera sinerae* were visualised in samples fixed in Lugol's solution, and their abundance was estimated by optical microscopy as described above for dinoflagellate counts.

Cysts of *Alexandrium minutum*. The life cycle of *A. minutum* comprises the formation of 2 types of cysts (Figuerola et al. 2007): the resting cysts (sexual stage) and the pellicle cysts (ecdysal stage). The resting cysts are double-walled, have an almost hemispherical appearance in frontal view and appear kidney shaped in lateral view (Bolch et al. 1991). Pellicle cysts lack the morphological characteristics of resting cysts and germinate faster (i.e. in about 24 h) when under the same environmental conditions. Pellicle cysts of this species may resemble the vegetative cells in samples fixed in Lugol's solution. However, a subsequent staining with Calcofluor White M2R stain (Fritz & Triemer 1985) allows for visual discrimination between the 2 cellular forms. The fluorochrome specifically binds to the cellulose that constitutes the external wall of the vegetative cells and thus allows distinguishing those cysts that do not exhibit fluorescence.

We also monitored the presence of *Alexandrium minutum* resting cysts and whether their abundance

was modified by the treatments. At the end of the experiments, the cultures were concentrated down to a final 50 ml volume. Resting cysts were visualised by optical microscopy in live samples with no additional staining.

Statistics. Statistical analyses were performed using Systat 11 for PC (Systat Software). Comparison of treatments over time for the different parameters was done using the nonparametric Kruskal–Wallis test (Motulsky 2003).

Model description. Although a great amount of literature exists on the population dynamics of parasite–host interactions, including a wide range of models, none of these models seemed to be suitable for situations of algal parasitism (Bruning et al. 1992). Thus, we adapted a system of equations typically used to describe harmful algal bloom dynamics (Truscott 1995, Franks 1997) to characterise parasite infection. The population dynamics is expressed through the following set of ordinary differential equations for the susceptible (S) and infected (I) individuals:

$$\frac{dS(t)}{dt} = r \cdot S(t) \left(1 - \frac{S(t)}{K}\right) - a \cdot I(t) \frac{[S(t)]^2}{k_I^2 + [S(t)]^2} \quad (2)$$

$$\frac{dI(t)}{dt} = b \cdot a \cdot I(t) \frac{[S(t)]^2}{k_I^2 + [S(t)]^2} - M \cdot I(t) \quad (3)$$

where t is the time in days and r is the maximum growth rate in the absence of the parasite. K represents the carrying capacity of the culture, defined as the maximum dinoflagellate abundance that can be attained in the absence of the parasite. K and r are intrinsic characteristics in each experiment. The maximum infection rate a gives the number of newly infected cells per time and present sporangia (which after opening liberate the free living zooids). The parameter k_I denotes a half-saturation constant for infection which governs how quickly the maximum infection rate is attained as the number of susceptible dinoflagellates increases. The proportionality coefficient b represents the fraction of infected dinoflagellates that are detected as mature sporangia at a given time. This factor accounts for our inability to recognise infected cells during the early stages of infection (see above). In the absence of mature sporangia, these cells are counted as susceptible. In the model we assumed that 10% ($b = 0.1$) of infected cells show mature sporangia and can thus be recognised as infected. This assumption is partly based on a suite of tests we conducted for a range of different parameter values for b which produced the best match between the model and the data for the chosen value of $b = 0.1$. We cannot say with certainty, however, whether this is a good or even realistic value, as there are no data in the literature in reference to this parameter. Finally, M is the

rate at which mature sporangia open and liberate the free-living swimming parasites. A full summary of all model parameters and their values for the particular simulations is provided in Table 1.

We applied the model from Eqs. (2) and (3) to Expts II & III in order to obtain estimates for the effect of turbulence on the different parameters. Expt I was excluded from the simulations because of the low dinoflagellate abundances in the inoculum (see above). S_0 corresponds to the initial count of susceptible cells at time $t = 0$. As we did not detect any mature sporangia at the beginning of the experiments, I_0 was set to 1 sporangium ml^{-1} (see ‘Results’). This value is well below the detection limit (200 % confidence limits, Venrick 1978a,b) of the microscopic estimation of cells used in our study. In order to constrain some of the model parameters, we estimated the range for the possible dinoflagellate growth rate r and carrying capacity K from the experiments (see Fig. 2e,f,h,i). Based on earlier work, we also assumed that the value of r under turbulent conditions should be ~75 % of the corresponding value in still conditions (Bolli et al. 2007, Llaveria et al. 2009). By varying the other parameters to obtain a best possible fit to the data using the maximum likelihood method, and assuming that the model

provides a sufficiently good representation of the underlying dynamics of the system (which we tested by means of a correlation analysis, cf. Table 1), this method was used to provide an objective means to estimate the effect of turbulence on some of the free parameters, in particular the maximum infection rate a .

Although the experiments lasted more than 15 d, we only used the first 9 d of each experiment for the comparison with the model simulations (3 initial days under still conditions plus 6 subsequent days either under still or turbulent conditions). By using only this shorter time period we tried to minimise the risk of dinoflagellate mortality induced by long exposure to high agitation (Llaveria et al. 2009).

RESULTS

Development of the natural bloom event

On the days preceding the sampling for Expt I, the natural phytoplankton community in Arenys de Mar Harbour was dominated by diatoms (mainly *Chaetoceros* spp., data not shown), which were still dominant on 28 February, the day when the inoculum for Expt I

Table 1. Model parameters and their values during the numerical simulations. The term ‘cells’ refers to susceptible vegetative cells; ‘spor’ corresponds to the mature sporangia. The 2 different values for a and k_I represent the 2 model realisations R1 and R2 that were examined (see ‘Results’ and Fig. 6). RMS: root mean square

Symbol	Meaning	Unit	Values used in the numerical simulations			
			Expt II		Expt III	
			Still	Turbulent	Still	Turbulent
r	Maximum growth rate in the absence of the parasite	d^{-1}	0.47	0.35	0.69	0.53
M	Rate of mature sporangia opening	d^{-1}	0.43	0.43	0.43	0.43
a (R1)	Maximum infection rate	Infected cells $\text{spor}^{-1} \text{d}^{-1}$	20.1	15.0	24	17
a (R2)			15	15	18	18
b	Mature sporangia fraction coefficient	Spor infected cells $^{-1}$	0.1	0.1	0.1	0.1
k_I (R1)	Half-saturation constant	Cells ml^{-1}	3000	3000	3500	3500
k_I (R2)			1850	3300	2350	4100
K	Carrying capacity	Cells ml^{-1}	5600	5600	6150	19000
S_0	Initial susceptible abundance	Cells ml^{-1}	2100	2100	1030	1030
I_0	Initial mature sporangia abundance	Spor ml^{-1}	1	1	1	1
r^2 (R1)	Model–data correlation for $S(t)$	-	0.97	1.00	0.94	0.97
r^2 (R2)			($p = 0.003$)	($p = 8 \times 10^{-5}$)	($p = 0.001$)	($p = 0.002$)
r^2 (R1)	Model–data correlation for $I(t)$	-	0.92	0.97	0.92	0.97
r^2 (R2)			($p = 0.009$)	($p = 0.001$)	($p = 0.01$)	($p = 0.002$)
r^2 (R1)	Model–data correlation for $I(t)$	-	0.90	0.99	0.92	0.99
r^2 (R2)			($p = 0.05$)	($p = 0.007$)	($p = 0.04$)	($p = 0.006$)
σ_S (R1)	Model–data RMS (Eq. 4) for $S(t)$	Cells ml^{-1}	0.92	0.99	0.94	0.99
σ_S (R2)			($p = 0.04$)	($p = 0.005$)	($p = 0.03$)	($p = 0.006$)
σ_I (R1)	Model–data RMS (Eq. 4) for $I(t)$	Cells ml^{-1}	224	363	410	716
σ_I (R2)			382	297	482	759
σ_I (R1)	Model–data RMS (Eq. 4) for $I(t)$	Cells ml^{-1}	37	9	99	36
σ_I (R2)			38	22	104	56

was obtained (Fig. 1). In the days after this first sample was taken, the natural succession led to a dinoflagellate-dominated community with similar abundances and temporal dynamics of *Alexandrium minutum* and *Scrippsiella trochoidea*, and lower but constant concentrations of *Prorocentrum micans* (Fig. 1). From the temporal evolution of cell numbers (Fig. 1), we can assume that the inocula for the 3 experiments were obtained at times that corresponded to the beginning (28 February), the early maintenance (10 March), and late maintenance/starting decay (29 March) phases of the dinoflagellate bloom.

Cellular abundances of the most common dinoflagellate species (*Prorocentrum micans*, *Alexandrium minutum* and *Scrippsiella trochoidea*)

The populations in each of the replicates in Expts I, II & III showed a very similar behaviour with only slight differences in cell numbers (Fig. 2). The 2 different

kinds of treatments produced significant differences in the cell abundances in all 3 experiments. The species-specific response to the treatments is summarised in the following paragraphs:

***Prorocentrum micans*:** During the first 3 d of the experiment, when both the Turbulent and Still flasks were at rest, all flasks showed similar cell abundances. After Day 3, when the agitation was started, the cell numbers in the shaken flasks were consistently lower in all 3 experiments compared to the still controls (Fig. 2a–c).

***Alexandrium minutum*:** In Expt I, the population showed a lag phase of 5 d (Fig. 2d) followed by a minor increase in cell numbers both in the Still and Turbulent treatments. Differences in the cellular abundances between the 2 treatments were not detected until the last day, when cell numbers started to drop in the Still cultures. Expts II and III exhibited a markedly different behaviour between the 2 treatments, with the Still populations collapsing on Days 9 and 7, respectively. A drop in cell numbers under turbulent conditions was

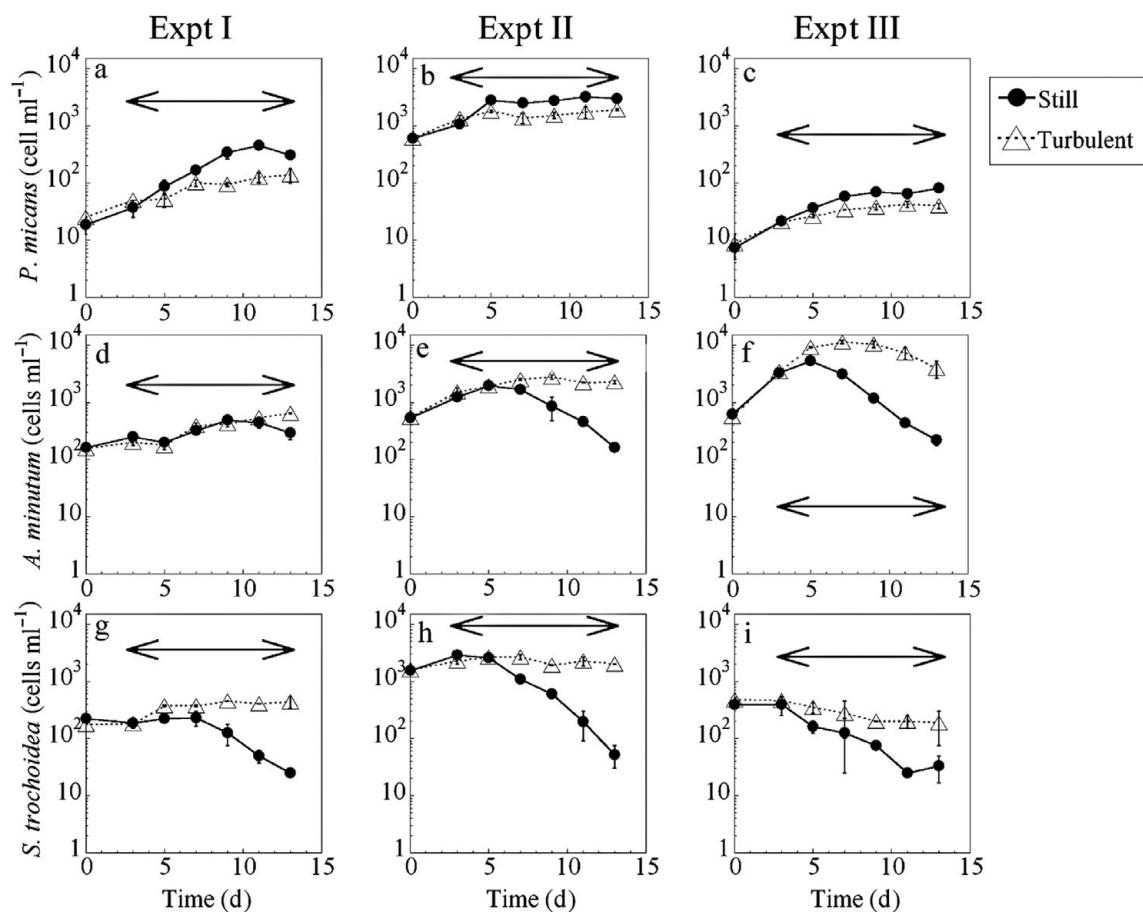


Fig. 2. *Prorocentrum micans*, *Alexandrium minutum*, and *Scrippsiella trochoidea*. Temporal evolution of the 3 most common dinoflagellate species during Expts I, II & III. Data points: averages of duplicates \pm SE. Double-ended horizontal arrows indicate the periods during which the corresponding flasks were placed on the orbital shaker

only detected in Expt III from Day 8 onwards (Fig. 2f), well before turning off the agitation. The decrease in cell numbers due to turbulence was less pronounced, however, compared to the decrease in the Still treatment. Overall, it appears that turbulence did not produce an increase in cell numbers but facilitated the maintenance of the population at a relatively high level, while the Still treatment always produced a drop in cell abundance (Fig. 2d–f).

***Scrippsiella trochoidea*:** In this species, the differences between the Turbulent and Still treatments resembled those observed in *Alexandrium minutum*: the cell numbers did not increase with turbulence, but the collapse of the population was prevented or at least delayed (Fig. 2g–i). In the Still treatment of Expts I, II and III, the populations started to collapse on Days 9, 7 and 5, respectively. In the last experiment (Fig. 2i), the populations subjected to turbulence exhibited a gradual but steady decrease in cell concentrations.

We also observed that the vertical cell distributions within the flasks were markedly different between the Still and Turbulent conditions. While the Turbulent treatments produced almost homogeneous cell distributions, in Still conditions, ~80% of the entire dinoflagellate population was concentrated in ca. 40 mm surface layers during certain hours of the day.

Infectivity of *Parvilucifera sinerae*

At the beginning of each experiment, we observed only healthy dinoflagellates with intact nuclei and protoplasm but no mature sporangia (i.e. infected cells). From Day 3 onwards, infected cells of *Alexandrium minutum* (Fig. 3a) and *Scrippsiella trochoidea* (Fig. 3b) were identified in all treatments. In contrast, we did not find any infected cells of *Prorocentrum micans*. At advanced stages of infection, the cells were morphologically disrupted, with a dark and degraded cytoplasm, broken thecae were abundant and *A. minutum* and *S. trochoidea* cells became difficult to distinguish from one another.

In general, the infectivity maximum coincided with a strong decrease in dinoflagellate cell numbers (Fig. 4). In Expts I and II, the infectivity was significantly reduced under turbulent conditions (Fig. 4a,b, Mann-Whitney U -test = 87.0; $p = 0.005$, $n = 20$ in Expt I, and U -test = 95.0; $p = 0.001$, $n = 20$ in Expt II). In Expt III, this trend was also observed until Day 9, but it reversed afterwards (Fig. 4c), when the decline of cell numbers in the shaken flasks coincided with the infectivity maximum. It was worth noting that in Expt III, the susceptible dinoflagellate population attained the highest level, more than 10^4 cells ml^{-1} , on Day 7 (Fig. 4c).

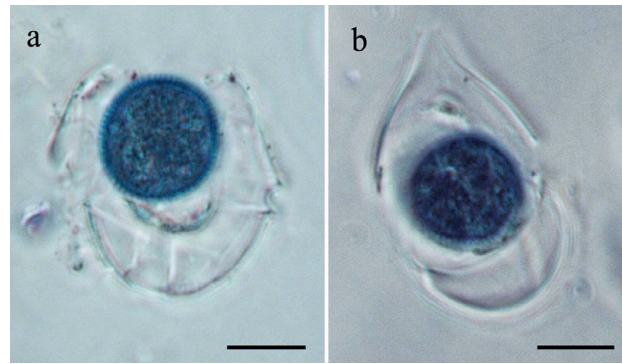


Fig. 3. *Parvilucifera sinerae*. Sporangial morphology as seen by light microscopy in (a) *Alexandrium minutum* and (b) *Scrippsiella trochoidea*. Scale bar: 10 μm

Alexandrium minutum cyst dynamics

The inoculum in Expt I had a higher proportion of pellicle cysts than those of Expts II and III (Fig. 5a–c). This feature might have been related to the longer manipulation of the field sample (screening process) to obtain the inocula for Expt I (see Materials and Methods and Discussion). Once the experiments started, in all Still treatments, the percentage of pellicle cysts decreased during the first 5 d and started to increase again afterwards. In contrast, in all experiments, turbulence significantly decreased the proportion of *A. minutum* pellicle cysts along the shaking period (Figs. 5a–c, Expt I: U -test = 100.0, $p = 0.000$, $n = 20$; Expt II: U -test = 100.0, $p = 0.000$, $n = 20$; and Expt III: U -test = 93.0, $p = 0.001$, $n = 20$), and their percentage never exceeded 30% of the total under turbulent conditions. The percentage of resting cysts formed at the end of the experiments did not account for more than the 1% of the total cell numbers, and the abundances did not depend on whether the cells were exposed to turbulence (data not shown). Thus, hereafter we will only refer to pellicle cysts.

Numerical simulations

We used the model from Eqs. (2) and (3) to simulate the temporal evolution of the number of susceptible (S) and infected (I) dinoflagellate cells in our experiments.

A comparison between the model and observed values is presented in Fig. 6, while Table 1 contains a summary of the parameter values. We were able to fit the model to the data using 2 very distinct realisations (R1 and R2). In the first realisation (R1), the model was

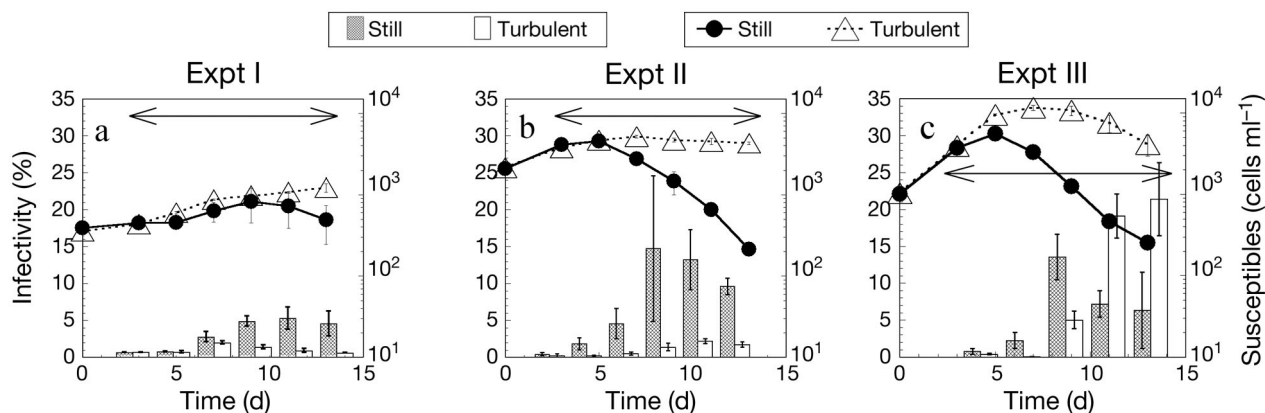


Fig. 4. Temporal evolution of the estimated infectivity in each experiment (bars, left ordinate) and temporal evolution of the number of susceptible cells (lines, right ordinate) during Expts I, II and III. All data are averages of the duplicates \pm SE. The double-ended horizontal arrows show the periods during which turbulence was applied to the corresponding flasks

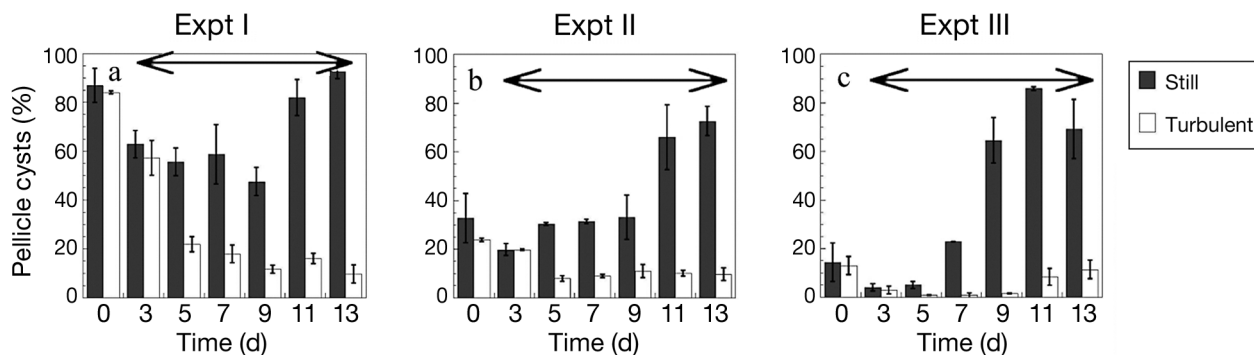


Fig. 5. Temporal changes in cyst abundances in Expts I, II and III in both treatments. Error bars indicate the SE of the mean. The double-ended horizontal arrows show the periods during which turbulence was applied to the corresponding flasks

fit to the data allowing for different infectivity rates, a , in the Still and Turbulent treatments. This resulted in a values that were between 25 and 30% lower under Turbulent conditions (Table 1). In the second realisation (R2), the infectivity rate was kept the same for both treatments. Nevertheless, we were able to produce a good fit to the data (cf. Fig. 6) using the maximum likelihood method if we allowed for different half-saturation concentrations, k_I (see Table 1 for all parameter values).

To quantify the ability of the model to fit the data, we used the root mean square (RMS) difference between the model prediction P and the data value D :

$$\sigma = \sqrt{(P - D)^2} \quad (4)$$

Finally, in both model set-ups, the values reached after long periods of exposure to the parasite [$S(t)$ and $I(t)$ for $t > 50$ d] tended towards the same steady state values for the Turbulent and Still treatments (not shown).

DISCUSSION

The main outcomes of this study are: (1) small-scale turbulence can decrease or delay the infection of *Alexandrium minutum* and *Scrippsiella trochoidea* by the parasite *Parvilucifera sinerae*; (2) these effects varied with the bloom phases (likely associated with different physiological states) and with the cell density of the host; (3) the modelling exercise suggested that turbulence could delay the parasite infection either by decreasing the maximum infection rate a and/or by increasing the half saturation constant k_I ; over a long term, turbulence would be unable to prevent infection.

The dynamics of the dinoflagellate populations showed different trends under Still and Turbulent conditions. The 3 species did not exhibit a marked increase in cell numbers when exposed to shaking, which agrees with findings by previous studies on monospecific cultures without parasites (Berdalet & Estrada 1993, Llaveria et al. 2009). During the few days

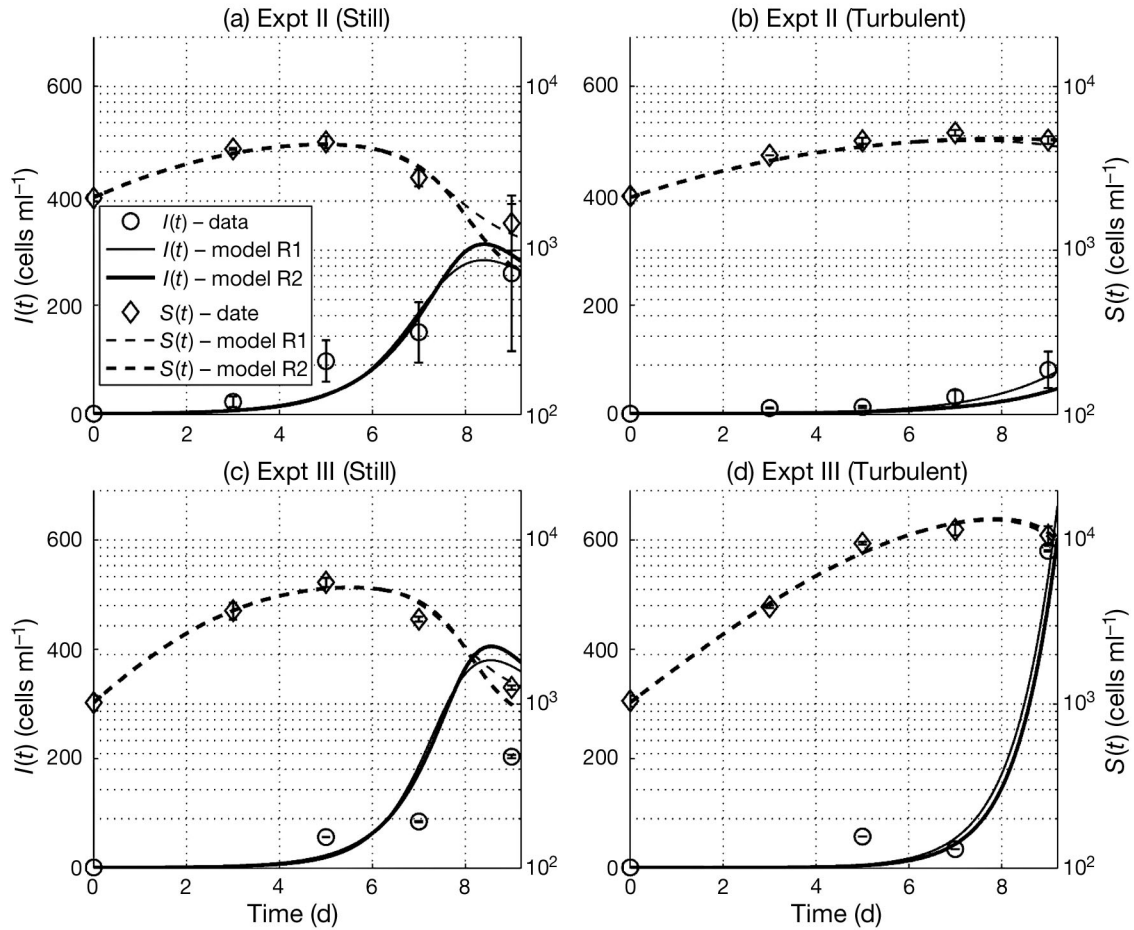


Fig. 6. Model-data comparison for Expts II & III using the parameter values from Table 1. Error bars are SE

of exposure to turbulence, the cell abundances of *Alexandrium minutum* and *Scrippsiella trochoidea* remained relatively constant. Unexpectedly, the populations of these 2 species decreased (with the degree of decay depending on the experiment) and collapsed under still conditions. It could be possible that a raise in pH may have occurred in the unshaken flasks, associated with the development of the microplanktonic communities. Havskum & Hansen (2006) noted that moderate turbulence could palliate pH-related growth limitations in high-density cultures of *Heterocapsa* sp. by facilitating gas exchange. Unfortunately, pH was not measured in the present work, and it is therefore not possible to evaluate the real contribution of this factor on the observed trends. Because 2 of our species were susceptible to parasitic infection, with high infectivity always coinciding with a sharp decline in cell numbers, it is more likely that the decay of our populations under still conditions was controlled by the presence of the parasite *Parvilucifera sinerae* rather than increased pH. This hypothesis is partially supported by

the observation that *Prorocentrum micans*, a species resistant to infection, grew better in still conditions than under turbulence.

Small-scale turbulence could interfere with the parasite infection through multiple mechanisms. Although turbulence can enhance the encounter rates (Rothschild & Osborn 1988), it may also shorten the period of contact between the host and parasite. As a consequence, relatively still conditions facilitate the host detection and penetration by the parasite. Moreover, if the host detection by this parasite depended on chemical signals (as in other parasites, e.g. Kühn & Hofmann 1999), it would be likely that turbulence eroded the chemical microzones surrounding the host cells (Jackson 1987), as has been observed in other processes (e.g. Mitchell et al. 1985, Alldredge & Cohen 1987, Wolfe 2000).

The rate of infection also depends on the host abundance and the host survival threshold at which the parasite starts to outgrow and decimate the host population (Bruning 1991, Holfeld 1998). In turn, the resulting

detection rate by the parasite strongly depends on the abundance and the degree of patchiness of the host (Park et al. 2004, Ostfeld et al. 2005), and aggregates may facilitate the appearance of infection foci around an initially infected cell (Real & Biek 2007). In our study, we found that dinoflagellates were able to perform vertical migrations under still conditions, forming near-surface accumulations in the experimental flasks at particular times of the diel cycle. Field observations showed that phytoplankton can aggregate in thin layers of high cell concentrations which form through a combination of physical and biological mechanisms (e.g. Birch et al. 2008). Our observations and modelling results suggest that the parasite infection of dinoflagellates could be promoted by the occurrence of layers of preferential concentration, while it might be hampered if the population is well mixed by turbulence and thus more disperse. Expt II provided an estimate of the host abundance required for an effective parasite infection. We estimated that about 80 % of the entire dinoflagellate population was concentrated in ca. 40 mm surface layers during certain hours of the day. In these layers, the cell concentrations would increase up to 10^4 cells ml^{-1} , about twice the average concentration in the flask. This concentration could be used as an estimate for the threshold that limits the efficient prevention of the infection by turbulence (Fig. 4c). Indeed, when cell concentrations were very high (e.g. towards the end of Expt III, the average concentration in the flasks exceeded 10^4 cells ml^{-1}), turbulence could no longer prevent the infection.

In order to help our understanding of the effect of turbulence on the different parameters that govern infection, we applied a simple infectivity model (Eqs. 2 & 3) to the data obtained from Expts II & III. The results from this exercise suggest that the observed differences in cell abundances under turbulent and still conditions (Fig. 2) can be explained with differences in the infection rate a . We found that turbulence could have decreased the infection rate a by ~25 to 30 % compared to still conditions (realisation R1 in Table 1 and Fig. 6). An equally good fit to the data could be obtained, however, by keeping the infection rate a the same for the Turbulent and Still treatments while increasing the half-saturation constant in the turbulent cultures. This simply has the effect that a higher concentration of host cells is required to achieve the same rate of infection. These results thus provided 2 possible explanations for how the infection process could be affected by turbulence: (1) turbulence acts to reduce the maximum infection rate a , or (2) under increased turbulence, the parasites require a higher concentration of host cells to achieve the same maximum infection rate. Both mechanisms lead to the same end result of a lower or delayed infection.

To fit the model to the data in Expt III under Turbulent conditions, the model required a value for the carrying capacity K that was about 3 times as high compared to the Still treatment (cf. Table 1). While the responsible mechanism behind this increase is unclear, we could hypothesise that turbulence could have negatively affected 1 or several of the other organisms present in the natural sample that act as direct competitors to (or grazers of) our species of interest, which would therefore grow better and thus achieve a higher carrying capacity. However, as we did not record cell counts for the other species present in the natural sample, this explanation remains speculative.

In both model set-ups, the steady states for long periods of exposure to the parasite [$S(t)$ and $I(t)$ for $t > 50$ d] tend to show similar values for the Turbulent and Still treatments, which suggests that turbulence only retards the infection but does not prevent it. To verify this hypothesis, further experiments are needed, including observations over longer time periods. Due to the negative effect of turbulence itself on cell mortality (Llave-ria et al. 2009), however, this might require a slightly different set-up that produces lower turbulence intensities that do not affect cell mortality.

The 3 experiments were performed with natural assemblages obtained during different phases of a dinoflagellate bloom. Thus, very likely the sampled populations were not in the same physiological state, which may superimpose on the observed effects of turbulence. In the succession from Expt I to III, the collapse of susceptible species in still conditions occurred increasingly early. In addition, Expt I was performed with communities from the initial (i.e. diatom dominated) phase of the spring bloom, that had the lowest host abundances. The level of infection of *Alexandrium minutum* by *Parvilucifera sinerae* in the Still treatments of this experiment was the lowest compared to the other 2 experiments. Overall, this may be due to the population being in a physiologically healthier state and/or caused by the lower host abundance, which reduces the capacity of the parasite to spread. From our data we could estimate that about 3000 cells ml^{-1} represents the lower concentration threshold for an effective infection by the parasite. The existence of such a threshold can only be hypothesised, however, and further studies would be necessary to support this hypothesis.

It has been postulated that certain life cycle stages could be an effective protection for dinoflagellates against parasitism. For instance, in cultures of *Alexandrium ostenfeldii*, the abundances of pellicle cysts augmented concurrently with a decrease in the infection by *Parvilucifera infectans* (Toth et al. 2004). In contrast, Figueroa et al. (2008) observed that pellicle cysts of *A. minutum* did not prevent infection by *P. sinerae*. At the

beginning of our 3 experiments, the percentage of cysts did not directly relate to the initial infectivity rates but to the manipulation of the natural sample (see 'Materials and methods'). In fact, the different proportion of pellicle cysts at Time 0 could be a result of the particular duration of the screening process of the field sample to achieve the suitable initial dinoflagellate concentration in the inocula. Expt I required a longer manipulation given that the sample was obtained from a diatom-dominated phytoplankton community. Once the experiment started, the proportion of cysts decreased in all flasks during the first 5 d, likely indicating a trend to recover the vegetative cell population. Thereafter, turbulence induced a marked reduction in the proportion of *A. minutum* pellicle cysts, as observed previously under similar experimental conditions (Bolli et al. 2007). In contrast, the Still treatment again increased the proportion of pellicle cysts, which could be related to the entrance on what could be called a stationary phase. High abundances of pellicle cysts occurred in the Still treatments, also with high infectivity levels. Only few pellicle cysts were present in the shaken flasks having lower levels of infection, except at the end of Expt III. Overall, our data are insufficient to make any conclusive statement on whether the formation of pellicle cysts is an effective strategy to prevent parasite infection.

Figueroa et al. (2008) noted that the infectivity of *Alexandrium minutum* by *Parvilucifera sinerae* was strain-specific while *Scrippsiella trochoidea* was resistant to such infection in both laboratory and natural populations. It could be hypothesised that the susceptibility of *S. trochoidea* to infection by *P. sinerae* is also strain-specific, but further studies would be needed to support or disprove this hypothesis. This observation would corroborate the concept of high specificity of host-parasite interactions (Chambouvet et al. 2008), however, and make it more difficult to design a possible control of harmful dinoflagellate blooms by parasitic attack (Anderson 1997). In any case, the results from the present study suggest that such a control could be modulated by turbulence.

Acknowledgements. This study was supported by the Spanish funded projects TURDITOX (CTM2005-03547/MAR), TURECOTOX (CTM2006-13884-C02-00/MAR; endorsed by GEOHAB, www.geohab.info) and PARAL (CTM2009-08399). G.L. held an FPU fellowship from the Spanish Ministry of Science and Education (SMSE). O.N.R. was a JAE-postdoctoral fellow of the CSIC and is currently a Marie Curie fellow (FP7 IEF proposal no. 255396). The work of R.F. and E.G. was supported by 'I3P' and 'Ramon y Cajal' postdoctoral contracts, respectively, of the SMSE. We thank the Agència Catalana de l'Aigua (ACA, Departament de Medi Ambient, Generalitat de Catalunya) for its cooperation in providing information from the monitoring program. We are grateful to all referees, whose critical comments and questions improved the quality and clarity of the manuscript.

LITERATURE CITED

- Alcaraz M (1997) Copepods under turbulence: grazing, behavior and metabolic rate. *Sci Mar* 61:177–195
- Allredge AL, Cohen Y (1987) Can microscale chemical patches persist in the sea? Microelectrode study of marine snow, fecal pellets. *Science* 235:689–691
- Anderson DM (1997) Bloom dynamics of toxic *Alexandrium* species in the northeastern U.S. *Limnol Oceanogr* 42:1009–1022
- Arin L, Marrasé C, Maar M, Peters F, Sala MM, Alcaraz M (2002) Combined effects of nutrients and small-scale turbulence in a microcosm experiment. I. Dynamics and size-distribution of osmotrophic plankton. *Aquat Microb Ecol* 29:51–61
- Balech E (1995) The genus *Alexandrium* Halim (Dinoflagellata). Sherkin Island Marine Station, Sherkin Island Co., Cork
- Berdalet E, Estrada M (1993) Effects of turbulence on several phytoplankton species. In Smayda TJ, Shimizu TSY (eds) Toxic phytoplankton blooms in the sea. Developments in marine biology, 5th Int Conf Toxic Mar Phytoplankton, Rhode Island, USA. Elsevier, New York, p 737–740
- Berdalet E, Estrada M (2005) Effects of small-scale turbulence on the physiological functioning of marine algae. In: Durvasula SR (ed) Algal cultures, analogues and applications. Science Publishers, Enfield, NH, p 459–500
- Berdalet E, Peters F, Koumandou L, Roldán C, Guadayol Ò, Estrada M (2007) Species-specific physiological response of dinoflagellates to quantified small-scale turbulence. *J Phycol* 43:965–977
- Birch DA, Young WR, Franks PJ (2008) Thin layers of plankton: formation by shear and death by diffusion. *Deep-Sea Res I* 55:277–295
- Bolch CJ, Blackburn SI, Cannon JA, Hallegraeff GM (1991) The resting cyst of the red-tide dinoflagellate *Alexandrium minutum* (Dinophyceae). *Phycologia* 30:215–219
- Bolli L, Llaveria G, Garcés E, Guadayol Ò, van Lenning K, Peters F, Berdalet E (2007) Modulation of ecdysal cyst and toxin dynamics of two *Alexandrium* (Dinophyceae) species under small-scale turbulence. *Biogeosciences* 4:559–567
- Bravo I, Figueroa RI, Garcés E, Fraga S, Massanet A (2010) The intricacies of dinoflagellate pellicle cysts: the example of *Alexandrium minutum* cysts from a bloom-recurrent area (Bay of Baiona, NW Spain). *Deep-Sea Res II* 57:166–174
- Bruning K (1991) Infection of the diatom *Asterionella* by a chytrid. 2. Effects of light on survival and epidemic development of the parasite. *J Plankton Res* 13:119–129
- Bruning K, Lingeman R, Ringelberg J (1992) Estimating the impact of fungal parasites on phytoplankton populations. *Limnol Oceanogr* 37:252–260
- Chambouvet A, Morin P, Marie D, Guillou L (2008) Control of toxic marine dinoflagellate blooms by serial parasitic killers. *Science* 322:1254–1257
- Doggett MS, Porter D (1996) Fungal parasitism of *Synedra acus* (Bacillariophyceae) and the significance of parasite life history. *Eur J Protistol* 32:490–497
- Estrada M, Berdalet E (1997) Phytoplankton in a turbulent world. *Sci Mar* 61(Suppl 1):125–140
- Figueroa RI, Garcés E, Bravo E (2007) Comparative study between the life cycles of *Alexandrium tamutum* and *Alexandrium minutum* (Gonyaulacales, Dinophyceae) in culture. *J Phycol* 43:1039–1053
- Figueroa RI, Garcés E, Massana R, Camp J (2008) Description, host-specificity, and strain selectivity of the dinofla-

- gellate parasite *Parvilucifera sinerae* sp. nov. (Perkinsozoa). *Protist* 159:563–578
- Franks PJS (1997) Models of harmful algal blooms. *Limnol Oceanogr* 42:1273–1282
- Fritz L, Triemer RE (1985) A rapid simple technique utilizing Calcofluor White M2R for the visualization of dinoflagellate thecal plates. *J Phycol* 21:662–664
- Guadayol O, Peters F, Stiansen JE, Marrasé C, Lohrmann A (2009) Evaluation of oscillating grids and orbital shakers as means to generate isotropic and homogeneous small-scale turbulence in laboratory enclosures commonly used in plankton studies. *Limnol Oceanogr Methods* 7:287–303
- Guillard RRL (1975) Culture of phytoplankton for feeding marine invertebrates. In: Smith W, Chanley MH (eds) *Culture of marine invertebrates*. Plenum, New York, NY, p 26–60
- Havskum H, Hansen PJ (2006) Net growth of the bloom-forming dinoflagellate *Heterocapsa triquetra* and pH: why turbulence matters. *Aquat Microb Ecol* 42:55–62
- Holfeld H (1998) Fungal infections of the phytoplankton: seasonality, minimal host density, and specificity in a mesotrophic lake. *New Phytol* 138:507–517
- Jackson GA (1987) Simulating chemosensory responses of marine microorganisms. *Limnol Oceanogr* 32:1253–1266
- Kim MC, Yoshinaga I, Imai I, Nagasaki K, Itakura S, Ishida Y (1998) A close relationship between algicidal bacteria and termination of *Heterosigma akashiwo* (Raphidophyceae) blooms in Hiroshima Bay, Japan. *Mar Ecol Prog Ser* 170:25–32
- Kjørboe T (1993) Turbulence, phytoplankton cell size and structure of pelagic food webs. *Adv Mar Biol* 29:1–72
- Kjørboe T, Visser AW (1999) Predator and prey perception in copepods due to hydromechanical signals. *Mar Ecol Prog Ser* 179:81–95
- Kühn SF, Hofmann M (1999) Infection of *Coscinodiscus granii* by the parasitoid nanoflagellate *Pirsonia diadema*: III. Effects of turbulence on the incidence of infection. *J Plankton Res* 21:2323–2340
- Llaveria G, Figueroa RI, Garcés E, Berdalet E (2009) Cell cycle and cell mortality of *Alexandrium minutum* (Dinophyceae) under small-scale turbulence conditions. *J Phycol* 45:1106–1115
- Maar M, Arin L, Simó R, Sala MM, Peters F, Marrasé C (2002) Combined effects of nutrients and small-scale turbulence in a microcosm experiment. II. Dynamics of organic matter and phosphorus. *Aquat Microb Ecol* 29:63–72
- Mackenzie BR, Miller TJ, Cyr S, Leggett WC (1994) Evidence for a dome-shaped relationship between turbulence and larval fish ingestion rates. *Limnol Oceanogr* 39:1790–1799
- Margalef R (1978) Life-forms of phytoplankton as survival alternatives in an unstable environment. *Oceanol Acta* 1: 493–509
- Mitchell JG, Okubo A, Fuhrman JA (1985) Microzones surrounding phytoplankton form the basis for a stratified marine microbial ecosystem. *Nature* 316:58–59
- Montagnes DJS, Chambouvet A, Guillou L, Fenton A (2008) Responsibility of microzooplankton and parasite pressure for the demise of toxic dinoflagellate blooms. *Aquat Microb Ecol* 53:211–225
- Motulsky H (2003) Prism 4 statistics guide—statistical analyses for laboratory and clinical researchers. GraphPad Software, San Diego, CA
- Nishitani L, Erickson G, Chew KK (1985) Role of the parasitic dinoflagellate *Amoebophrya ceratii* in control of *Gonyaulax catenella* populations. In: Anderson DM, White AW, Baden DG (eds) *Toxic dinoflagellates*. Elsevier Science Publishers, New York, p 225–230
- Norén F, Moestrup Ø, Rehnstam-Holms AS (1999) *Parvilucifera infectans* Noren et Moestrup gen. et sp. nov. (Perkinsozoa phylum nov.): a parasitic flagellate capable of killing toxic microalgae. *Europ J Protistol* 35: 233–254
- Ostfeld RS, Glass GE, Keesing F (2005) Spatial epidemiology: an emerging (or reemerging) discipline. *Trends Ecol Evol* 20:328–336
- Park MG, Yih W, Coats DW (2004) Parasites and phytoplankton, with special emphasis on dinoflagellate infections. *J Eukaryot Microbiol* 51:145–155
- Peters F, Marrasé C (2000) Effects of turbulence on plankton: an overview of experimental evidence and some theoretical considerations. *Mar Ecol Prog Ser* 205:291–306
- Real LA, Biek R (2007) Spatial dynamics and genetics of infectious diseases on heterogeneous landscapes. *J R Soc Interface* 4:935–948
- Rothschild BJ, Osborn TR (1988) Small-scale turbulence and plankton contact rates. *J Plankton Res* 10:465–474
- Saiz E, Alcaraz M, Paffenhofer GA (1992) Effects of small-scale turbulence on feeding rate and gross-growth efficiency of three *Acartia* species (Copepoda: Calanoida). *J Plankton Res* 14:1085–1097
- Steidinger KA, Tangen K (1997) Dinoflagellates. In: Tomas CR (ed) *Identifying marine phytoplankton*. Academic Press, St Petersburg, FL, p 387–584
- Thronsdon J (1995) Estimating cell numbers. In: Hallegraeff GM, Anderson DM, Cembella AD (eds) *Manual on harmful marine microalgae*. IOC manuals and guides No. 33, p 63–80. UNESCO, Paris
- Toth GB, Selander E, Norén F, Pavia H (2004) Marine dinoflagellates show induced life-history shifts to escape parasite infection in response to water-borne signals. *Proc Biol Sci* 271:733–738
- Truscott JE (1995) Environmental forcing of simple plankton models. *J Plankton Res* 17:2207–2232
- Utermöhl H (1958) Zur Vervollkommnung der quantitativen Phytoplankton-Methodik. *Mitt Int Ver Limnol* 9:1–38
- Van Lenning K, Vila M, Masó M, Garcés E, Anglès S, Sampeiro N, Morales-Blake A, Camp J (2007) Short-term variations in development of a recurrent toxic *Alexandrium minutum*-dominated dinoflagellate bloom induced by meteorological conditions. *J Phycol* 43:892–907
- Venrick EL (1978a) How many cells to count? In: Sournia A (ed) *Monographs on oceanographic methods 6: phytoplankton manual*. UNESCO, Paris, p 167–180
- Venrick EL (1978b) Statistical considerations. In: Sournia A (ed) *Monographs on oceanographic methods 6: phytoplankton manual*. UNESCO, Paris, p 238–250
- Vila M, Camp J, Garcés E, Masó M, Delgado M (2001) High resolution spatio-temporal detection of potentially harmful dinoflagellates in confined waters of the NW Mediterranean. *J Plankton Res* 23:497–514
- Wolfe GV (2000) The chemical defense ecology of marine unicellular plankton: constraints, mechanisms, and impacts. *Biol Bull (Woods Hole)* 198:225–244